

Research Article

Phase Reversal Technique Applied to Fishnet Metalenses

Victor Pacheco-Peña ¹, Igor V. Minin ², Oleg V. Minin,² and Miguel Beruete ^{3,4}

¹*Emerging Technology and Materials Group, School of Engineering, Newcastle University, Merz Court, Newcastle upon Tyne NE1 7RU, UK*

²*National Research Tomsk State University, Tomsk 634050, Russia*

³*Antennas Group-TERALAB, Universidad Pública de Navarra, Campus Arrosadía, 31006 Pamplona, Spain*

⁴*Institute of Smart Cities (ISC), Public University of Navarre, Campus Arrosadía, 31006 Pamplona, Spain*

Correspondence should be addressed to Victor Pacheco-Peña; victor.pacheco-pena@newcastle.ac.uk and Miguel Beruete; miguel.beruete@unavarra.es

Received 13 April 2018; Revised 2 July 2018; Accepted 11 July 2018; Published 26 August 2018

Academic Editor: Shah Nawaz Burokur

Copyright © 2018 Victor Pacheco-Peña et al. This is an open access article distributed under the Creative Commons Attribution License, which permits unrestricted use, distribution, and reproduction in any medium, provided the original work is properly cited.

In this work, the fishnet metamaterial is applied to several converging metalenses by combining the zoning, reference phase, and phase reversal techniques. First, the zoning and reference phase techniques are implemented in several metalenses at 55 GHz ($\lambda_0 = 5.45$ mm) with a short focal length of $1.5\lambda_0$. Then, the phase reversal technique is applied to these metalenses by switching from a concave to a convex profile in order to change the phase distribution inside of them. The designs are evaluated both numerically and experimentally demonstrating that chromatic dispersion (the shift of the position of the focus at different frequencies) is reduced when using the phase-reversed profiles. It is shown how the position of the focus remains at the same location within a relatively broadband frequency range of $\sim 4\%$ around the design frequency without affecting the overall behaviour of the metalenses. The best performance is achieved with the design that combines both reference phase and phase reversal techniques, with an experimental position of the focus of $1.75\lambda_0$, reduced side lobes, and a power enhancement of 6.5 dB. The metalenses designed here may find applications in situations where a wideband response and low side lobes are required because of the reduced chromatic aberrations of the focus.

1. Introduction

Metamaterials (MTMs) are artificial structures engineered to get control of light propagation beyond the possibilities offered by natural materials [1–4]. One of the first groundbreaking applications of metamaterials was the perfect lens proposed by Pendry in 2000 [5], and since then, many other enhanced focusing devices have been proposed and implemented showing the benefits of applying MTMs within the entire electromagnetic (EM) spectrum. Some of the milestones in this discipline are superlenses and hyperbolic lenses [6, 7], superoscillatory lenses [8–10], advanced designs following transformation optics techniques [11–14], and even focusing devices based on extreme refractive index values [15–21]. Several techniques have been proposed to fulfill the specific needs of each spectral window. For instance, the

classical arrangement of SRR and wires has been widely used for lenses operating at microwaves [22, 23]. However, for higher frequencies, these structures are limited due to their increasing losses.

Among the large numbers of MTM structures reported in the past years, the fishnet has proven to provide a good performance for high-frequency and quasioptical applications [24–30]. It has been demonstrated that by designing a free-standing fishnet MTM with two in-plane periods, a very low-loss structure can be fabricated in the millimeter wave range [31, 32]. In addition, through manipulation of permittivity (ϵ) and permeability (μ), a plano-concave lens with good (ideally perfect) matching to free space can be obtained [33, 34].

A major drawback of the abovementioned lenses is the large volume occupied by the lens that leads to a considerable

weight of the structure. To mitigate this problem, one can apply the zoning technique whereby parts of the lens are removed when their phase variation with respect to free-space propagation is an integer multiple of 2π [35–37]. This has been done in the past with the fishnet metalens reducing the concave profile significantly without penalizing seriously the performance [38–40]. More sophisticated techniques borrowed from Fresnel lenses can be proposed to enhance the performance of the zoned fishnet metalenses such as application of a positive reference phase to reduce side lobes [41, 42].

In this paper, we continue this study by changing the typical concave profile to a convex profile; that is, we aim to evaluate the performance when the phase distribution inside the lens is reversed compared to the designs shown in [42]. In a previous letter [42], we showed that the best performance is achieved when a positive reference phase is used. In the present manuscript, we show the design and numerical and experimental results of two different convex profiles with a focal length (FL) of $1.5\lambda_0$ using $q=0$ and $q=0.35$ at a millimeter wave frequency of 55 GHz. As it will be demonstrated, the zoning technique along with the reference phase is used for the designs [41, 42]. The difference in the present work is that we aim to evaluate the performance of the lenses when the phase reversal technique is also applied. This is done by reversing the phase distribution inside of the lenses and changing its profile from concave to convex. Hence, the designed metamaterial lenses consist of a combination of the three techniques: zoning, reference phase, and phase reversal. As it will be shown, by reversing the profile of the metalenses, the chromatic aberration (i.e., the shift of position of the focal length (FL) at different frequencies around the designed one) is reduced, as compared to the concave profiles. Moreover, a relatively broadband operational frequency range of $\sim 4\%$ around the design frequency is achieved.

2. Design and Dispersion Diagram Results

The metalenses considered here use both the zoning technique and the reference phase. These were already explained in detail in [42], but the basics are briefly exposed here for completeness. The zoning technique consists in reducing the lens profile for a phase advance of 2π ; that is, every time the lens thickness reaches a maximum value $t = \lambda_0 / (1 - n_{\text{lens}})$, where λ_0 is the operation wavelength in free space and n_{lens} is the effective refractive index of the lens.

With the reference phase, an extra phase advance is allowed inside the lens [43, 44]. This additional phase is modulated between 0 and 2π , giving as a result a total phase that varies within the range $[0-4\pi]$. This means that the lens thickness has an increment compared to that of a lens without a reference phase that can be calculated as

$$\Delta t = q \frac{\lambda_0}{1 - n_{\text{lens}}}, \quad (1)$$

where Δt is the additional thickness due to the reference phase technique and q is a factor between 0 and 1 that

corresponds to an extra phase advance from 0 to 2π . So, for a lens with simultaneous zoning and reference phase techniques, the profile is reduced when a thickness $t_{\text{total}} = \Delta t + t$ is reached. Finally, the profile of the metalens is then

$$z = \text{mod} \left[\frac{\text{FL}(1 - n_{\text{lens}}) - \sqrt{\text{FL}^2(1 - n_{\text{lens}})^2 - x^2(1 - n_{\text{lens}})}}{1 - n_{\text{lens}}^2} \right],$$

$$t_{\text{total}} = t(q + 1), \quad (2)$$

where mod is the modulo operation.

The unit cell employed is the same as the one used in our previous paper [42] and is reproduced in the inset of Figure 1(a) for completeness. Its dimensions are $w = 0.35$ mm, $d_x = 3$ mm, $d_y = 5$ mm, $d_z = 1.35$ mm, and $a = 2.4$ mm. The metal layers are made of copper with conductivity $\sigma_{\text{Cu}} = 5.8 \times 10^7$ S/m and are separated by an air layer of thickness 1 mm ($d_z - w$). With these parameters, the effective refractive index of an infinite array of such unit cells was calculated using the Eigenmode solver of the commercial software CST Microwave Studio®. The results are shown in Figure 1(a).

From these results, we select an operation frequency of 55 GHz because it falls in the range where n_{lens} has a smooth variation so that the design is less sensitive to manufacturing tolerances and alignment. At this frequency, the refractive index has a magnitude $|n_{\text{lens}}| = 0.68$ which is a good trade-off because, according to (1), for very small $|n_{\text{lens}}|$, the first zone would be very thick. Moreover, since we are dealing with a small focal length (FL), from (2), the first zone is narrower and the lens profile becomes more abrupt. Therefore, we would need a narrower unit cell (along the x -axis, d_x) to discretize properly the lens profile.

Taking into account these factors, two metalenses were designed: without ($q=0$, Figure 1(b)) and with ($q=0.35$, Figure 1(c)) a reference phase. Due to the application of the phase reversal technique, the regions with air and the fishnet MTM are exchanged, and hence convex profiles are obtained. Notice that when $q=0$, only the phase reversal is applied to the metalens and when $q=0.35$, both the reference phase and phase reversal techniques are applied.

3. Results and Discussion

The focusing performance of the metalenses was evaluated both numerically and experimentally. The numerical simulations were carried out using the transient solver of CST Microwave Studio. In the first study, the focal position and the operation frequency in the numerical simulations were found by exciting the lens with a plane wave (with linear polarization, E_y) impinging normally on the flat face and recording the spectra at the output along the z -axis by means of point electric field probes. They were located at $0.2 \text{ mm} < z < 20 \text{ mm}$ with a step of 0.2 mm in order to accurately record the electric field along the propagation axis. The experimental characterization was performed using an ABmm™ VNA operating in the V-band of millimeter waves. The experimental setup is shown in Figure 2(a). A high gain

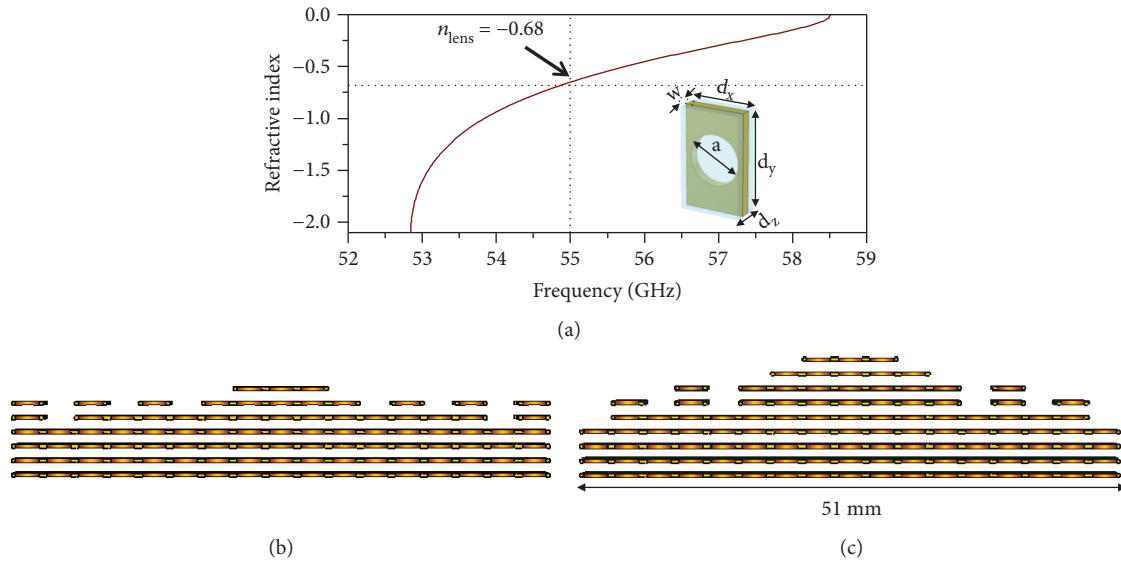


FIGURE 1: Dispersion diagram of the unit cell and profiles of the metalenses. (a) Refractive index of the fishnet structure used to design the lenses, assuming it to be infinitely periodic. Unit cell (inset) with dimensions: $d_x = 3$ mm, $d_y = 5$ mm, $d_z = 1.35$ mm, and $a = 2.4$ mm. The thickness of the metal is $w = 0.35$ mm. Top view of the schematic representation of the reversed-phase zoned fishnet metalenses with (b) $q = 0$ and (c) $q = 0.35$.

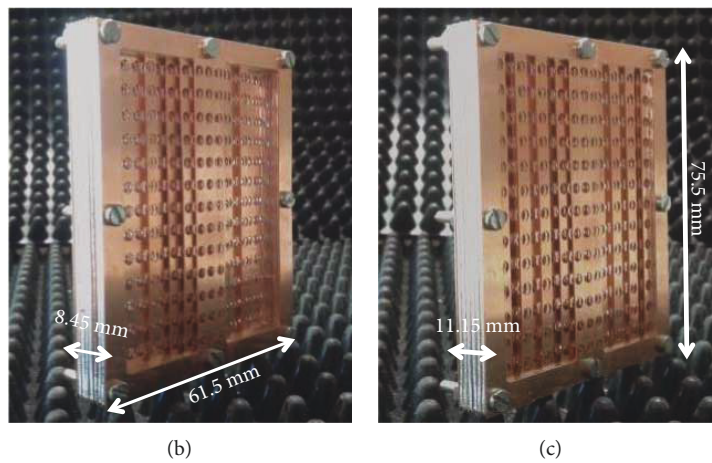
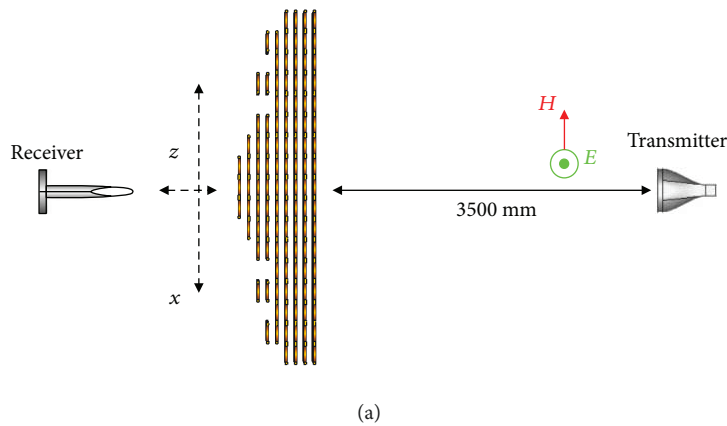


FIGURE 2: Fabricated prototypes. (a) Sketch of the experimental setup used for characterizing the metalenses. Photographs of the fabricated metalenses with (b) $q = 0$ and (c) $q = 0.35$, both with the phase reversal technique.

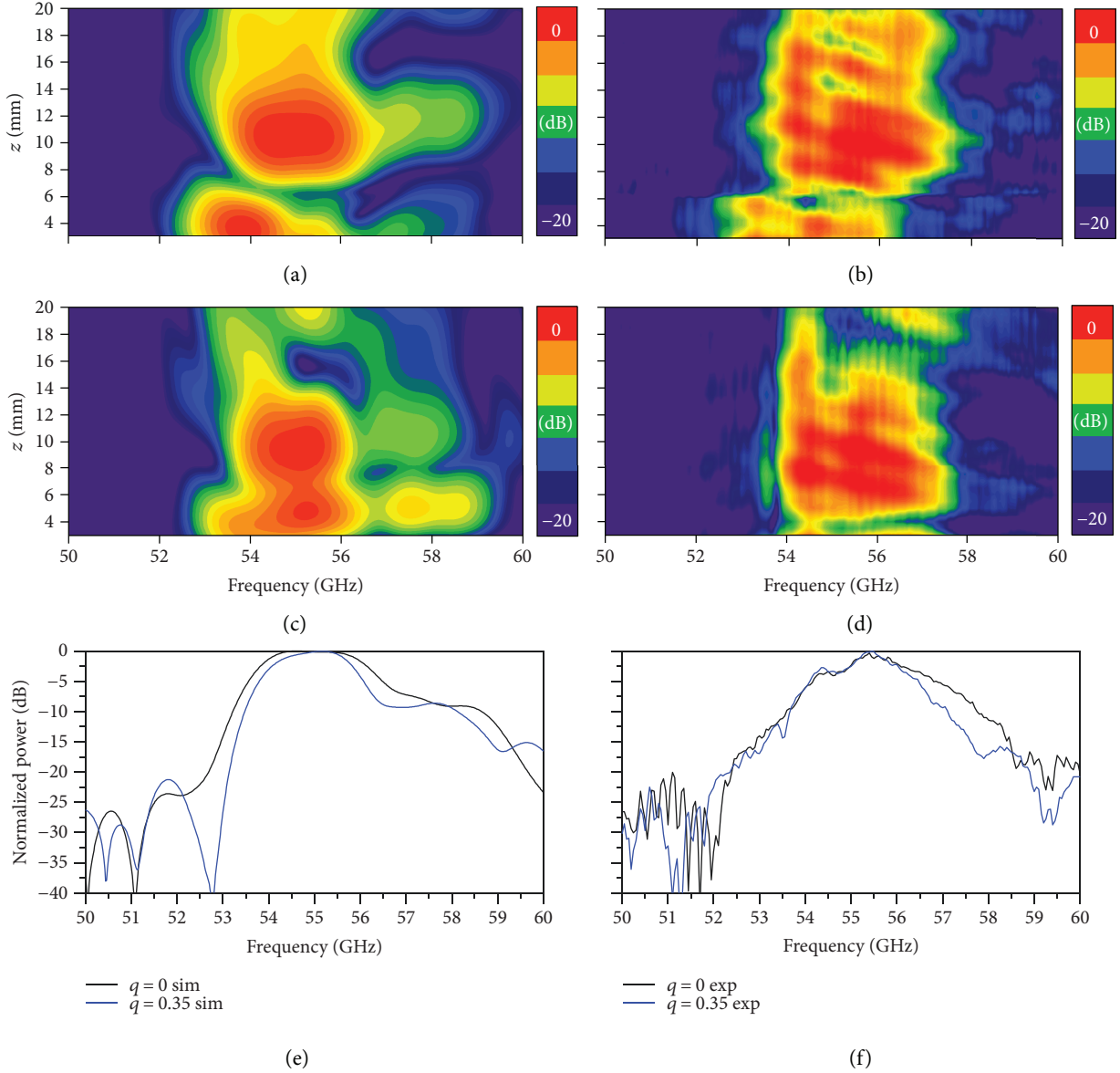


FIGURE 3: Spectral response. Numerical (a, c) and experimental results (b, d) of the power distribution spectra along the propagation z -axis for the phase reversal designs with $q=0$ (a, b) and $q=0.35$ (c, d). The simulation and experimental results of the spectral response of power distribution at each FL are shown in (e) and (f), respectively.

horn antenna was used as a transmitter. It was placed at 3500 mm from the flat face of the metalenses to ensure a uniform illumination. The transmitted power was scanned with an open-ended waveguide probe located on a translation stage to record the spectral response of the metalenses at each z position and determine both the position of the focus and the operation frequency. The photographs of the fabricated metalenses and their whole dimensions are presented in Figures 2(b) and 2(c) for the prototypes with $q=0$ and $q=0.35$, respectively. Note that they have the same thickness as the concave structures shown in [42] as expected because we have only exchanged the air-metal regions which results in a fixed volume of metalenses. Both lenses have 17×13 holes in

the transversal plane ($x \times y$), with total dimensions of $61.5 \text{ mm} \times 75.5 \text{ mm}$ (including the frame). As discussed in [26, 42], the number of plates at the input are critical to reproduce the refractive index of the infinite structure given that we are operating in the limit where n_{lens} has abrupt or smooth variations. Based on this, in the central part of the metalenses, we placed four plates with holes to have a performance similar to that of the ideal infinite fishnet MTM.

With this configuration, the results (numerical and experimental) of the normalized power distribution spectra along the z -axis for each design are shown in Figures 3(a)–3(d), respectively. In general, a good agreement is observed. Note that with these designs, the

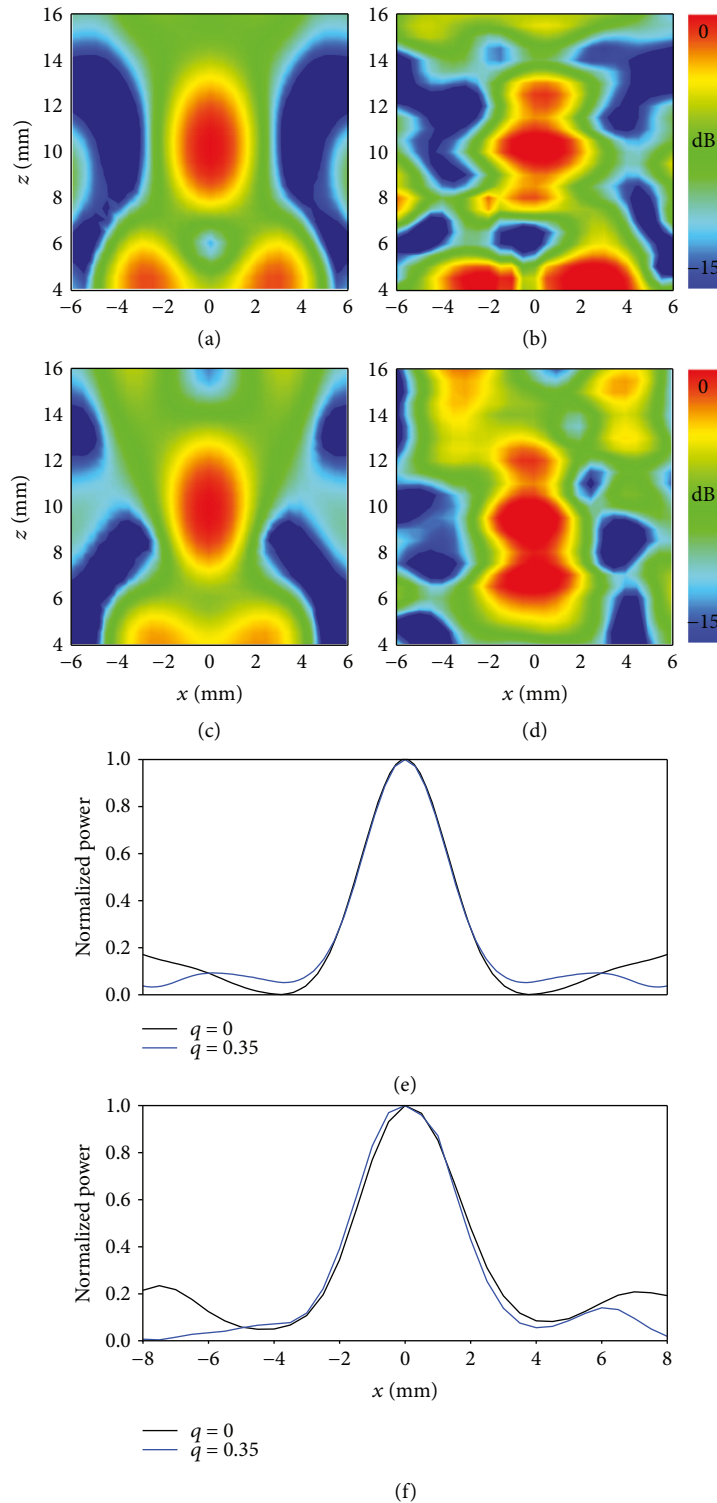


FIGURE 4: Focusing performance. Numerical (a, c, e) and experimental results (b, d, f) of the power distribution in the xz plane (H -plane) for the designs with phase reversal and reference phase with a value of $q = 0$ (a, b) and $q = 0.35$ (c, d). Numerical (e) and experimental (f) values of the normalized power along the transversal x -axis at each FL for the prototypes with phase reversal and $q = 0$ (black) and $q = 0.35$ (blue).

chromatic dispersion is reduced (i.e., the shifting of the focus when changing the operational frequency), as compared with the concave profiles, with the focus emerging at the same position even when the frequency is changed from 54 to 56 GHz which is a relatively broad bandwidth

of 2 GHz (~4%) considering the intrinsic narrow band response of the fishnet MTM [33, 45, 46]. Moreover, in the simulation, the peak of maximum power (focus) appears at the operation frequency (55 GHz) with FL = 10.25 mm ($1.87 \lambda_0$) and FL = 9.8 mm ($1.79 \lambda_0$) for $q = 0$

TABLE 1: Results of the focusing properties of the metalenses with reference phase and phase reversal. The experimental and numerical values are given at frequencies of 55.5 GHz and 55 GHz, respectively.

	$q = 0$		$q = 0.35$	
	Sim	Exp	Sim	Exp
FL	$1.87 \lambda_0$	$1.94 \lambda_0$	$1.79 \lambda_0$	$1.75 \lambda_0$
FWHMx	$0.55 \lambda_0$	$0.555 \lambda_0$	$0.54 \lambda_0$	$0.55 \lambda_0$
DF	$0.93 \lambda_0$	$0.925 \lambda_0$	$0.94 \lambda_0$	$0.97 \lambda_0$
Enh	5.7 dB	4.5 dB	8.2 dB	6.5 dB

and $q = 0.35$, respectively. In the experiment, the focus appears at 55.5 GHz with a FL = 10.5 mm ($1.94 \lambda_0$) and FL = 9.5 mm ($1.75 \lambda_0$), for each design, respectively. The slight deviation of the FL, $\sim 0.3 \lambda_0$ from the designed value ($1.5 \lambda_0$), along with the small frequency deviation (0.9%) in all the metalenses could be attributed to experimental misalignments and fabrication tolerances. Additionally, this small error could be due to the fact that the waves emerging from the furthest zones (along the x -axis) of a convex profile reach the focal plane at different positions along the z -axis, that is, spherical aberrations of the lens. However, we can consider that this deviation is small taking into account that the FL for each metalens is close to the design value. For the sake of completeness, the numerical and experimental results of the power distribution spectra at each FL are shown in Figures 3(e) and 3(f), respectively, demonstrating that the operational bandwidth is increased with these designs compared with the concave profiles.

For the sake of completeness, the impedance matching between the lenses and free space was numerically evaluated using the frequency domain solver of the commercial software CST Microwave Studio (not shown). In this study, the fishnet metamaterial was modeled using an infinite array of holes along the x - and y -axes considering 9 perforated plates along the propagation z -axis (which corresponds to the maximum number of plates used in the proposed lenses as shown in Figure 1). The effective ϵ and μ and normalized impedance η of the fishnet metamaterial were calculated from the S -parameters, giving as a result $\text{Re}\{\epsilon\} = -0.7$, $\text{Re}\{\mu\} = -0.38$, and $\eta = 0.75$ at the operation frequency of 55 GHz. Note that despite the fact that the proposed lenses are not perfectly matched with free space ($\eta = 1$), small reflections are still expected.

In the next study, the power distribution in the xz plane at the operation frequency and FL position for each metalens is found. In the simulation analysis, the results were found by defining a power density monitor at the operation frequency. In the experiment, a similar procedure was carried out to measure the focal plane: the receiving probe was placed on a translation stage and then moved from -6 to 6 mm and from 4 to 16 mm along the x -axis and z -axis with a step of 0.25 mm at the operation frequency. The results are shown in Figure 4. For the naked eye, the good agreement between both results with a clear focus produced by each structure is

evident. To better compare the focal properties, the numerical and experimental values of the power distribution along the transversal axis at each FL are presented in Figures 4(e) and 4(f), respectively, where again a good agreement is observed. Moreover, it is shown that the lateral lobes in the focal plane are reduced when $q = 0.35$ and the phase reversal technique is used, as expected [42]. A summary of the focal properties of these metalenses is shown in Table 1 in terms of the full width at half maximum (FWHM), FL, depth of focus along the z -axis (DF), and power enhancement at the FL.

As it is shown, the best performance is obtained for the design with $q = 0.35$ and phase reversal with a higher power enhancement, reduced FWHM, and an FL closer to the design value. By comparing these results with the concave counterparts [42], the metalenses with phase reversal suffer from spherical aberrations because the DF is increased compared with that in the concave structures, as explained before. However, these results demonstrate that convex metalenses with small FL can be also designed using the fishnet MTM. Moreover, they can be used in applications where a wideband response is needed due to the fact that these designs have a reduced chromatic aberration of the FL.

4. Conclusions

The profile of the zoned fishnet metalenses using the reference phase technique has been changed from a concave profile to a convex profile in order to evaluate their performance when the phase distribution inside of them is reversed. From the results of the spectral response, it has been shown that the chromatic dispersion is reduced with the reversed convex fishnet metalenses compared with the concave profiles. In this respect, it has been demonstrated that the position of the focus does not change for a relatively broadband frequency range of $\sim 4\%$ around the design frequency (considering the intrinsic narrow band response of the fishnet metamaterial) without affecting the overall performance of the metalenses. The best performance in terms of the power enhancement, reduced FWHM, and FL close to the design value has been achieved with the design with $q = 0.35$ which combines both the reference phase and phase reversal techniques. The metalenses designed here may find applications where a wideband response and low side lobes are needed due to the reduced chromatic aberrations of the focus.

Data Availability

The data used to support the findings of this study are available from the corresponding author upon request.

Conflicts of Interest

The authors declare that there is no conflict of interest regarding the publication of this paper.

Acknowledgments

The authors would like to thank Dr. V. Torres for the fabrication of the prototypes. This communication is based on the research conducted within the PhD thesis developed by Victor Pacheco-Peña. This work was partially supported by the Spanish Ministerio de Economía y Competitividad with European Union Fondo Europeo de Desarrollo Regional (FEDER) funds (TEC2014-51902-C2-2-R). Victor Pacheco-Peña is supported by Newcastle University (Newcastle University Research Fellow). Igor V. Minin and Oleg V. Minin were partially supported by the Mendeleev scientific fund of Tomsk State University.

References

- [1] N. Engheta and R. W. Ziolkowski, *Metamaterials: Physics and Engineering Explorations*, John Wiley & Sons, 2006.
- [2] C. Argyropoulos, F. Monticone, N. M. Estakhri, and A. Alù, "Tunable plasmonic and hyperbolic metamaterials based on enhanced nonlinear response," *International Journal of Antennas and Propagation*, vol. 2014, Article ID 532634, 11 pages, 2014.
- [3] J. P. Turpin, J. A. Bossard, K. L. Morgan, D. H. Werner, and P. L. Werner, "Reconfigurable and tunable metamaterials: a review of the theory and applications," *International Journal of Antennas and Propagation*, vol. 2014, Article ID 429837, 18 pages, 2014.
- [4] H. Chen, Q. Cheng, A. Huang et al., "Modified Luneburg lens based on metamaterials," *International Journal of Antennas and Propagation*, vol. 2015, Article ID 902634, 6 pages, 2015.
- [5] J. B. Pendry, "Negative refraction makes a perfect lens," *Physical Review Letters*, vol. 85, no. 18, pp. 3966–3969, 2000.
- [6] N. Fang, H. Lee, C. Sun, and X. Zhang, "Sub-diffraction-limited optical imaging with a silver superlens," *Science*, vol. 308, no. 5721, pp. 534–537, 2005.
- [7] Z. Liu, H. Lee, Y. Xiong, C. Sun, and X. Zhang, "Far-field optical hyperlens magnifying sub-diffraction-limited objects," *Science*, vol. 315, no. 5819, p. 1686, 2007.
- [8] E. T. F. Rogers, J. Lindberg, T. Roy et al., "A super-oscillatory lens optical microscope for subwavelength imaging," *Nature Materials*, vol. 11, no. 5, pp. 432–5, 2012.
- [9] T. Roy, E. T. F. Rogers, and N. I. Zheludev, "Sub-wavelength focusing meta-lens," *Optics Express*, vol. 21, no. 6, pp. 7577–7582, 2013.
- [10] S. Legaria, V. Pacheco-Peña, and M. Beruete, "Performance enhancement of binary Fresnel lenses using metamaterials," in *The 11th International Congress on Engineered Material Platforms for Novel Wave Phenomena, Metamaterials 2017*, Marseille, France, 2017.
- [11] D.-H. Kwon and D. H. Werner, "Beam scanning using flat transformation electromagnetic focusing lenses," *IEEE Antennas and Wireless Propagation Letters*, vol. 8, pp. 1115–1118, 2009.
- [12] R. Yang, W. Tang, and Y. Hao, "A broadband zone plate lens from transformation optics," *Optics Express*, vol. 19, no. 13, pp. 12348–12355, 2011.
- [13] A. Demetriadou and Y. Hao, "Slim Luneburg lens for antenna applications," *Optics Express*, vol. 19, no. 21, pp. 19925–19934, 2011.
- [14] A. Demetriadou and Y. Hao, "A grounded slim Luneburg lens antenna based on transformation electromagnetics," *IEEE Antennas and Wireless Propagation Letters*, vol. 10, pp. 1590–1593, 2011.
- [15] T. Driscoll, D. N. Basov, A. F. Starr et al., "Free-space microwave focusing by a negative-index gradient lens," *Applied Physics Letters*, vol. 88, no. 8, article 081101, 2006.
- [16] M. J. Freire, R. Marques, and L. Jelinek, "Experimental demonstration of a $\mu=-1$ metamaterial lens for magnetic resonance imaging," *Applied Physics Letters*, vol. 93, no. 23, article 231108, 2008.
- [17] V. Torres, V. Pacheco-Peña, P. Rodríguez-Ulibarri et al., "Terahertz epsilon-near-zero graded-index lens," *Optics Express*, vol. 21, no. 7, pp. 9156–9166, 2013.
- [18] C. Della Giovampaola and N. Engheta, "Digital metamaterials," *Nature Materials*, vol. 13, no. 12, pp. 1115–1121, 2014.
- [19] V. Torres, B. Orzabayev, V. Pacheco-Peña et al., "Experimental demonstration of a millimeter-wave metallic ENZ lens based on the energy squeezing principle," *IEEE Transactions on Antennas and Propagation*, vol. 63, no. 1, pp. 231–239, 2015.
- [20] V. Pacheco-Peña, M. Navarro-Cía, and M. Beruete, "[INVITED] epsilon-near-zero metalenses operating in the visible: invited paper for the section: hot topics in metamaterials and structures," *Optics & Laser Technology*, vol. 80, pp. 162–168, 2016.
- [21] V. Pacheco-Peña, N. Engheta, S. Kuznetsov, A. Gentshev, and M. Beruete, "Experimental realization of an epsilon-near-zero graded-index metalens at terahertz frequencies," *Physical Review Applied*, vol. 8, no. 3, 2017.
- [22] C. G. Parazzoli, R. B. Gregor, J. A. Nielsen et al., "Performance of a negative index of refraction lens," *Applied Physics Letters*, vol. 84, no. 17, pp. 3232–3234, 2004.
- [23] R. B. Gregor, C. G. Parazzoli, J. A. Nielsen, M. A. Thompson, M. H. Tanielian, and D. R. Smith, "Simulation and testing of a graded negative index of refraction lens," *Applied Physics Letters*, vol. 87, no. 9, article 091114, 2005.
- [24] S. Zhang, W. Fan, N. C. Panoiu, K. J. Malloy, R. M. Osgood, and S. R. J. Brueck, "Experimental demonstration of near-infrared negative-index metamaterials," *Physical Review Letters*, vol. 95, no. 13, 2005.
- [25] G. Dolling, C. Enkrich, M. Wegener, C. M. Soukoulis, and S. Linden, "Simultaneous negative phase and group velocity of light in a metamaterial," *Science*, vol. 312, no. 5775, pp. 892–894, 2006.
- [26] M. Beruete, M. Sorolla, and I. Campillo, "Left-handed extraordinary optical transmission through a photonic crystal of sub-wavelength hole arrays," *Optics Express*, vol. 14, no. 12, p. 5445, 2006.
- [27] C. García-Meca, R. Ortuño, F. J. Rodríguez-Fortuño, J. Martí, and A. Martínez, "Double-negative polarization-independent fishnet metamaterial operating in the visible spectrum," in *2009 IEEE/LEOS Winter Topicals Meeting Series*, pp. 83–84, Innsbruck, Austria, 2009.
- [28] C. García-Meca, R. Ortuño, F. J. Rodríguez-Fortuño, J. Martí, and A. Martínez, "Negative refractive index metamaterials aided by extraordinary optical transmission," *Optics Express*, vol. 17, no. 8, p. 6026, 2009.
- [29] S. Zhou, S. Townsend, Y. M. Xie, X. Huang, J. Shen, and Q. Li, "Design of fishnet metamaterials with broadband negative refractive index in the visible spectrum," *Optics Letters*, vol. 39, no. 8, pp. 2415–2418, 2014.

- [30] D. Tanasković, M. Obradov, O. Jakšić, and Z. Jakšić, "A low-loss double-fishnet metamaterial based on transparent conductive oxide," *Physica Scripta*, vol. T162, 2014.
- [31] M. Beruete, M. Sorolla, M. Navarro-Cía, F. Falcone, I. Campillo, and V. Lomakin, "Extraordinary transmission and left-handed propagation in miniaturized stacks of doubly periodic subwavelength hole arrays," *Optics Express*, vol. 15, no. 3, p. 1107, 2007.
- [32] B. Orazbayev, M. Beruete, V. Pacheco-Peña, G. Crespo, J. Teniente, and M. Navarro-Cía, "Soret fishnet metalens antenna," *Scientific Reports*, vol. 5, no. 1, p. 9988, 2015.
- [33] M. Beruete, M. Navarro-Cía, M. Sorolla, and I. Campillo, "Planoconcave lens by negative refraction of stacked sub-wavelength hole arrays," *Optics Express*, vol. 16, no. 13, p. 9677, 2008.
- [34] M. Navarro-Cía, M. Beruete, I. Campillo, and M. Sorolla, "Enhanced lens by ϵ and μ near-zero metamaterial boosted by extraordinary optical transmission," *Physical Review B*, vol. 83, no. 11, 2011.
- [35] W. E. Kock, "Metal-Lens Antennas," *Proceedings of the IRE*, vol. 34, no. 11, pp. 828–836, 1946.
- [36] P. F. Goldsmith, "Zone plate lens antennas for millimeter and submillimeter wavelengths," in *The Third International Symposium on Space Terahertz Technology: Symposium Proceedings*, pp. 345–361, Ann Arbor, MI, USA, 1992.
- [37] O. V. Minin and I. V. Minin, *Diffraction Optics of Millimeter Waves*, IOP Publisher, London, UK, 2004.
- [38] V. Pacheco-Peña, B. Orazbayev, V. Torres, M. Beruete, and M. Navarro-Cía, "Ultra-compact planoconcave zoned metallic lens based on the fishnet metamaterial," *Applied Physics Letters*, vol. 103, no. 18, article 183507, 2013.
- [39] V. Pacheco-Peña, B. Orazbayev, U. Beaskoetxea, M. Beruete, and M. Navarro-Cía, "Zoned near-zero refractive index fishnet lens antenna: steering millimeter waves," *Journal of Applied Physics*, vol. 115, no. 12, article 124902, 2014.
- [40] B. Orazbayev, V. Pacheco-Peña, M. Beruete, and M. Navarro-Cía, "Exploiting the dispersion of the double-negative-index fishnet metamaterial to create a broadband low-profile metallic lens," *Optics Express*, vol. 23, no. 7, pp. 8555–8564, 2015.
- [41] V. Pacheco-Peña, M. Navarro-Cía, B. Orazbayev, I. V. Minin, O. V. Minin, and M. Beruete, "Zoned fishnet lens antenna with reference phase for side-lobe reduction," *IEEE Transactions on Antennas and Propagation*, vol. 63, no. 8, pp. 3710–3714, 2015.
- [42] V. Pacheco-Peña, I. V. Minin, O. V. Minin, and M. Beruete, "On the performance of the zoned fishnet metamaterial lens with positive and negative reference phase," *IEEE Antennas and Wireless Propagation Letters*, vol. 16, pp. 1460–1463, 2017.
- [43] S. M. Stout-Grandy, A. Petosa, I. V. Minin, O. V. Minin, and J. Wight, "A systematic study of varying reference phase in the design of circular Fresnel zone plate antennas," *IEEE Transactions on Antennas and Propagation*, vol. 54, no. 12, pp. 3629–3637, 2006.
- [44] I. V. Minin and O. V. Minin, "Reference phase in diffractive lens antennas: a review," *Journal of Infrared, Millimeter, and Terahertz Waves*, vol. 32, no. 6, pp. 801–822, 2011.
- [45] M. Beruete, P. Rodriguez-Ulbarri, V. Pacheco-Peña, M. Navarro-Cía, and A. E. Serebryannikov, "Frozen mode from hybridized extraordinary transmission and Fabry-Perot resonances," *Physical Review B*, vol. 87, no. 20, article 205128, 2013.
- [46] V. Pacheco-Peña, *Metamaterials and plasmonics applied to devices based on periodic structures at high frequencies: microwave, terahertz and optical range*, [Ph.D. thesis], Public University of Navarra, 2016.



Hindawi

Submit your manuscripts at
www.hindawi.com

